

## Electronic Supplementary Information (ESI)

### Selective edge functionalization of graphene layers with oxygenated groups by means of Reimer-Tiemann and domino Reimer-Tiemann / Cannizzaro reactions

Vincenzina Barbera<sup>1\*</sup>, Luigi Brambilla<sup>1</sup>, Alessandro Porta<sup>1</sup>, Roberta Bongiovanni<sup>2</sup>, Alessandra Vitale<sup>2</sup>, Giulio Torrisi,<sup>1</sup> Maurizio Galimberti<sup>1\*</sup>

<sup>1</sup>Politecnico di Milano, Department of Chemistry, Materials and Chemical Engineering “G. Natta”, Via Mancinelli 7, 20131 Milano, Italy

<sup>2</sup>Politecnico di Torino, Department of Applied Science and Technology, Corso Duca degli Abruzzi 24, 10129 Torino, Italy

**Figure S1.** Reaction of G-OH with KOH and CHCl<sub>3</sub> performed at about 21°C as the nominal temperature (Procedure 1), a couple of seconds after G-OH addition.

**Figure S2.** High resolution XPS C<sub>1s</sub> peak and fitting curves for G-CHO and G-COOH.

**Table S1.** XPS C<sub>1s</sub> peak deconvolution and contribution assignment for HSAG, G-OH, G-COOH and G-CHO.

**Figure S3.** High resolution XPS O<sub>1s</sub> peak and fitting curves for G-CHO and G-COOH.

**S1.** Preparation of G-OH/HCHO mixture

**Figure S4.** FTIR spectrum of G-OH (a) and G-OH/HCHO (b) in the region 1800-700 cm<sup>-1</sup> after baseline correction.

**S2.** Control experiment: HSAG/CHCl<sub>3</sub>/KOH

**Figure S5.** FTIR spectra of HSAG (a) and HSAG/CHCl<sub>3</sub>/KOH (b) in the region 1800-700 cm<sup>-1</sup>.

**Figure S6.** Proposed synthetic pathway for the reaction of G-OH with CHCl<sub>3</sub>/KOH at room temperature: mechanism of Reimer-Tiemann (A) and Cannizzaro (B) reactions.

The reaction mechanism is discussed as follows.

**S3.** Functionalization yield of G-OH and G-CHO adducts

**Figure S7.** TGA curves of G-OH (a) and G-CHO (b).

**Table S2.** Mass loss for HSAG, G-OH and G-CHO adducts, from TGA analysis.

**Table S3.** Yield of functionalization for G-CHO.

**S4.** Stoichiometry of the domino Reimer-Tiemann / Cannizzaro process.

**Table S4.** Theoretical moles of functional groups in G-OH and G-COOH, assuming the occurring of domino Reimer-Tiemann / Cannizzaro process

**S5.** Reaction of G-OH with KOH / H<sub>2</sub>O / CHCl<sub>3</sub> at 0°C (Procedure 2)

**Figure S8.** FT-IR spectra of G-CHO-COOH (a) and G-CHO (b) in the region 1800-700 cm<sup>-1</sup> after baseline correction. Asterisks indicate absorptions assigned to 2-hydroxyaryl aldehyde functional groups.

**Figure S9.** XPS analysis of G-CHO-COOH: (a) wide scan spectra of G-CHO-COOH and G-CHO, (b) high resolution C<sub>1s</sub> peak and fitting curves for G-CHO-COOH, (c) high resolution O<sub>1s</sub> peak and fitting curves for G-CHO-COOH.

**Figure S10.** Proposed synthetic pathway for the reaction of G-OH with CHCl<sub>3</sub>/KOH at 0°C.

**S6.** Crosslinking of G-CHO with hexamethylenediamine

**Figure S11.** FTIR spectra of G-CHO (a), G-OH/HMA (b) and HMA (c) in the region 1800-700 cm<sup>-1</sup>.

**S7.** Cyclic Voltammetry (CV)

**Figure S12.** CVs of 0.1 M Et<sub>4</sub>NBF<sub>4</sub>/10 mM K<sub>4</sub>Fe(CN)<sub>6</sub> solution (a), 0.125 mM G-CHO suspension/0.1 M Et<sub>4</sub>NBF<sub>4</sub> (b) and 0.1 M Et<sub>4</sub>NBF<sub>4</sub>/10 mM K<sub>4</sub>Fe(CN)<sub>6</sub> solution and 0.125 mM G-CHO (c)



**Figure S1.** Reaction of G-OH with KOH and  $\text{CHCl}_3$  performed at about  $21^\circ\text{C}$  as the nominal temperature (Procedure 1), a couple of seconds after G-OH addition.

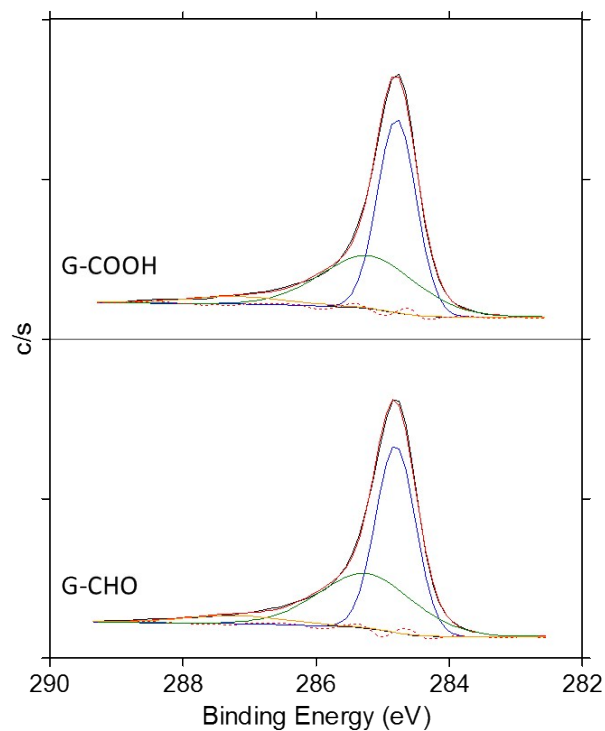


**Figure S2.** High resolution XPS  $C_{1s}$  peak and fitting curves for G-CHO and G-COOH.

**Table S1.** XPS  $C_{1s}$  peak deconvolution and contribution assignment for HSAG, G-OH, G-COOH and G-CHO.

	$C_{1s}$		
	C1	C2	C3
B.E. (eV)	284.8	285.2–285.7	287.2–287.8
Contribution	C $sp^2$	C-O	C=O

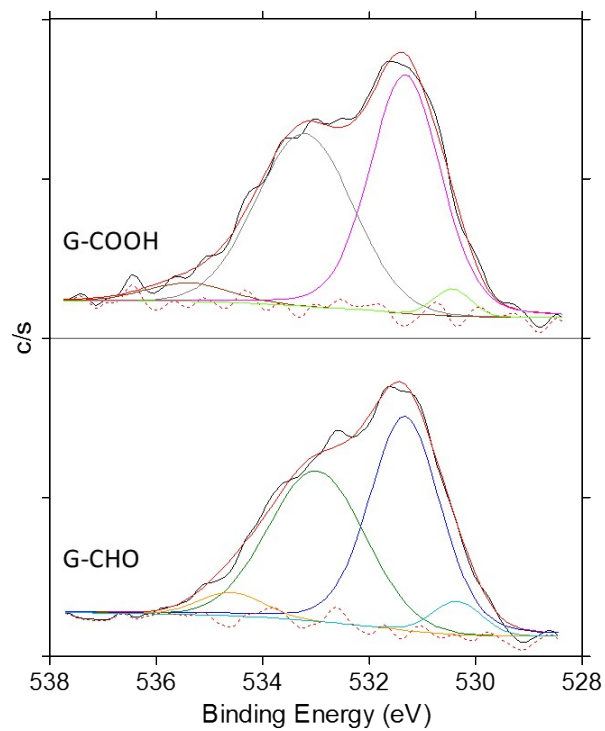


**Figure S3.** High resolution XPS O<sub>1s</sub> peak and fitting curves for G-CHO and G-COOH.

## S1. Preparation of G-OH/HCHO mixture

### *Experimental procedure*

In a 10 mL round bottomed flask a formaldehyde solution (37wt. % in H<sub>2</sub>O) stabilized with methanol, (41 mg, 1.4 mmol) and G-OH (100 mg) were added in sequence. The mixture was left to stir at room temperature for 12 hours and after analyzed by means of FTIR spectroscopy.

### *Characterization*

FT-IR spectrum was recorded, without observing any modification of G-OH (Figure S7).

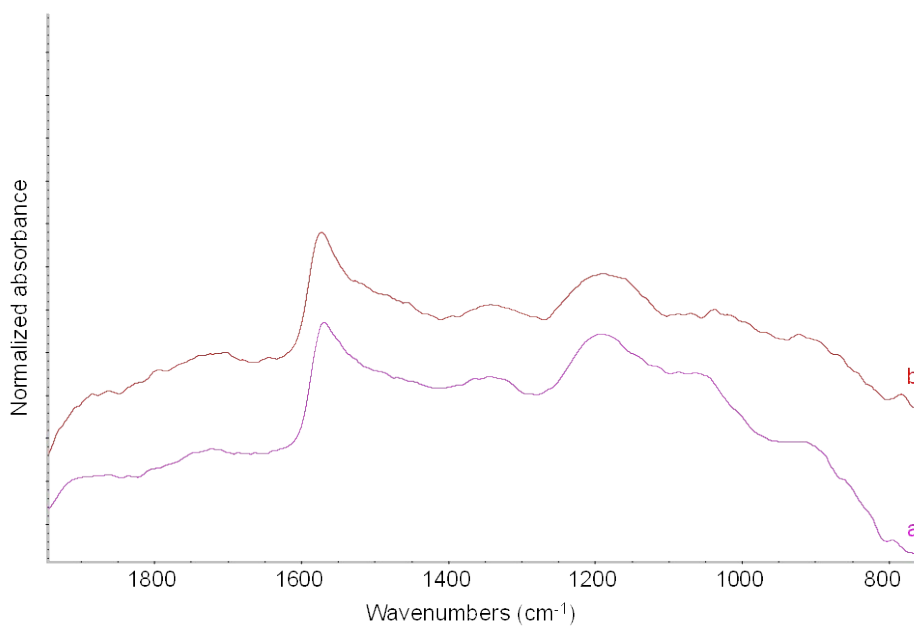


**Figure S4.** FTIR spectrum of G-OH (a) and G-OH/HCHO (b) in the region 1800-700 cm<sup>-1</sup> after baseline correction.

## S2. Control experiment: HSAG/CHCl<sub>3</sub>/KOH

### *Experimental procedure*

In a round bottomed flask equipped with magnetic stirrer and condenser, KOH powder (3.12 g, 55 mmol), HSAG (0.5 g) and H<sub>2</sub>O (0.5 mL) were added in sequence. CHCl<sub>3</sub> (1.12 mL, 14 mmol) was added to such mixture after few seconds in three parts (3 x 0.37 mL). The mixture was stirred at 0°C for 12 hours. After this time, solvent was removed at reduced pressure. The solid was reduced in fine grains in a mortar with a pestel, transferred into a Falcon™ tube (15mL) and water (10 mL) was added. The suspension was sonicated for 10 minutes and centrifuged at 4000 rpm for 10 minutes (3 times). 0.50 g of black powder were obtained.

### *Characterization*

Infrared spectrum is shown in Figure S5: typical spectral features of cyclopropane rings cannot be detected.

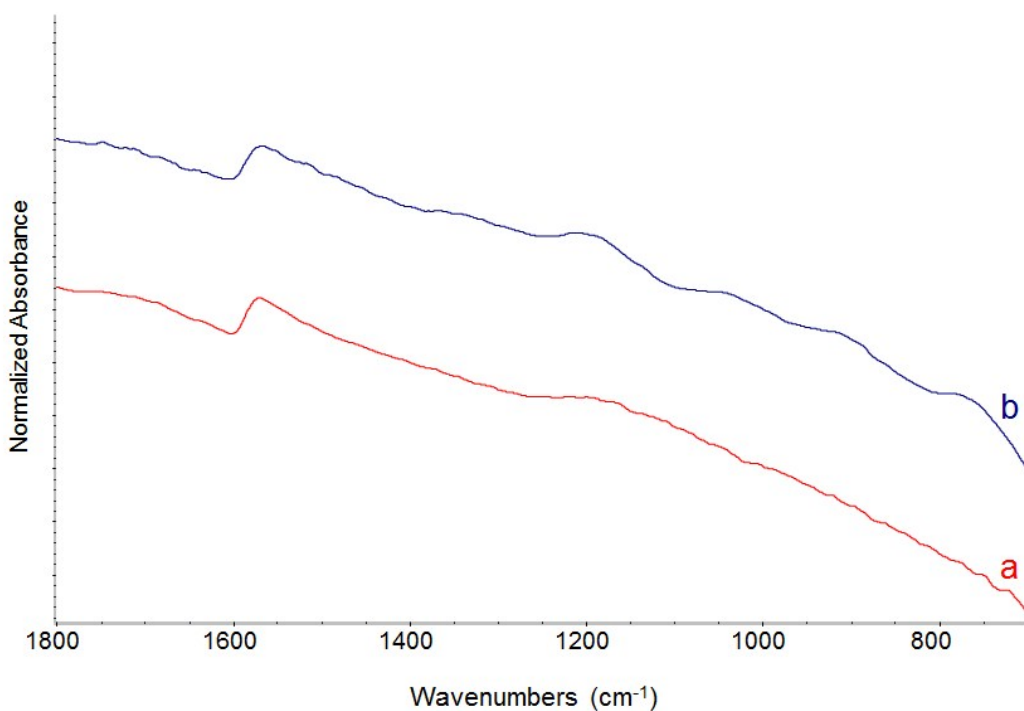


**Figure S5.** FTIR spectra of HSAG (a) and HSAG/CHCl<sub>3</sub>/KOH (b) in the region 1800-700 cm<sup>-1</sup>.

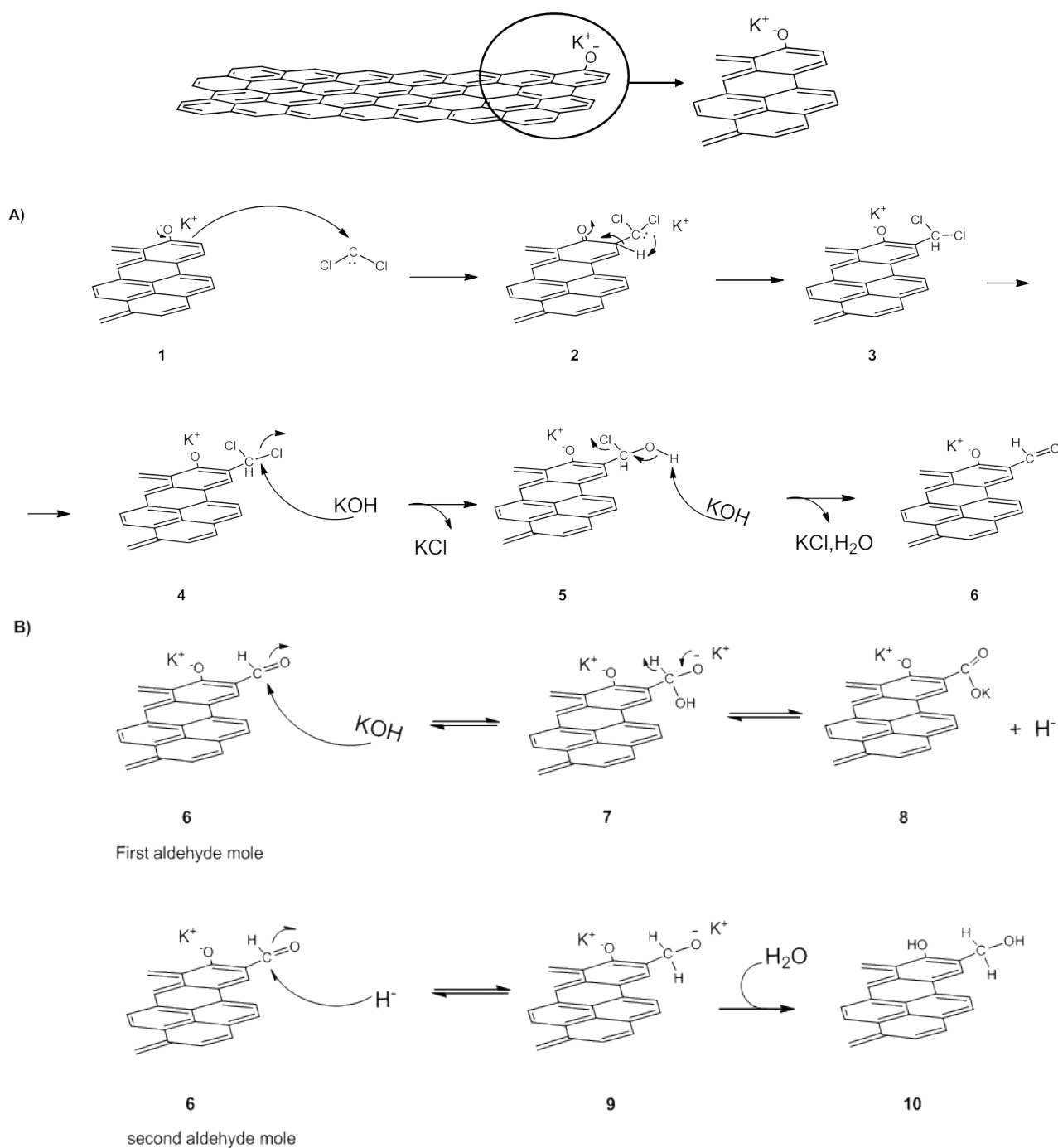


**Figure S6.** Proposed synthetic pathway for the reaction of G-OH with  $\text{CHCl}_3/\text{KOH}$  at room temperature: mechanism of Reimer-Tiemann (A) and Cannizzaro (B) reactions.

*Mechanism of Reimer-Tiemann reaction (Fig. S6A)*

Figure S6A shows the mechanism for the introduction on graphene layers of aldehyde functional groups, through the Reimer-Tiemann reaction. It is known that chloroform reacts with aqueous potassium phenoxide very slowly at room temperature, but its reactivity remarkably increases in the presence of a strong base such as  $\text{KOH}$  [54].  $\text{KOH}$  deprotonates  $\text{CHCl}_3$ , leading to a trichlorocarbanion, and deprotonates the OH groups on the graphene layer as well, forming product

1. The trichlorocarbanion, through a quick  $\alpha$ -elimination, spontaneously loses a chloride ion forming neutral dichlorocarbene, the reactive species that attacks **1**. The negatively charged phenoxide-like rings in **1**, with their negative charge delocalized on many aromatic rings, have a large resonance stabilization. Dichlorocarbene could react with both the phenoxide ion and the carbon atoms in the ortho positions with respect to the oxygenated group. Indeed, both mechanisms are reported in scientific literature [54]. Reactivity with ortho positions is favored by the charge delocalization which increases nucleophilicity of the carbon atoms. As a matter of fact, only this reactivity can account for the formation of an aldehydic species. Moreover, studies on the reactivity of dichlorocarbene in the Reimer-Tiemann reaction [54] demonstrated the quick formation of o- and p-hydroxybenzaldehydes. FT-IR findings suggested that dichlorocarbene attacks carbon atoms in ortho position with respect to aldehyde. Hence, dichlorocarbene gives rise to an attack on the ortho carbon atom of the phenoxide ion, forming product **3**, through the dichloro intermediate **2**. Such regioselective ortho attack, followed by 1,2-proton transfer, is the preferred mechanism [54], even though the intermolecular proton transfer mediated by water cannot be ruled out. Hydrolysis promoted by KOH leads to o-hydroxyformyl graphene layers, i.e. final product **6**, with CHO group in ortho position with respect to OH.

*Mechanism of Cannizzaro disproportionation (Fig. S6B)*

Product **6**, obtained through a Reimer-Tiemann reaction, undergoes a nucleophilic attack of the hydroxide ion on the aldehydic group. The tetrahedral carbon (intermediate **7**) expels a hydride ion becoming a potassium carboxylate group (product **8**). A second molecule of o-hydroxyformyl graphene **6** undergoes a nucleophilic acyl addition by the hydride ion. The benzyloxy intermediate **9** becomes alcohol (**10**) upon washing with water.

### S3. Functionalization yield of G-OH and G-CHO adducts

Thermogravimetric analysis was performed on HSAG, G-OH and G-CHO. TGA was performed under nitrogen. Thermographs of G-OH and G-CHO are shown in Figure S7. TGA of HSAG was already reported in [51].

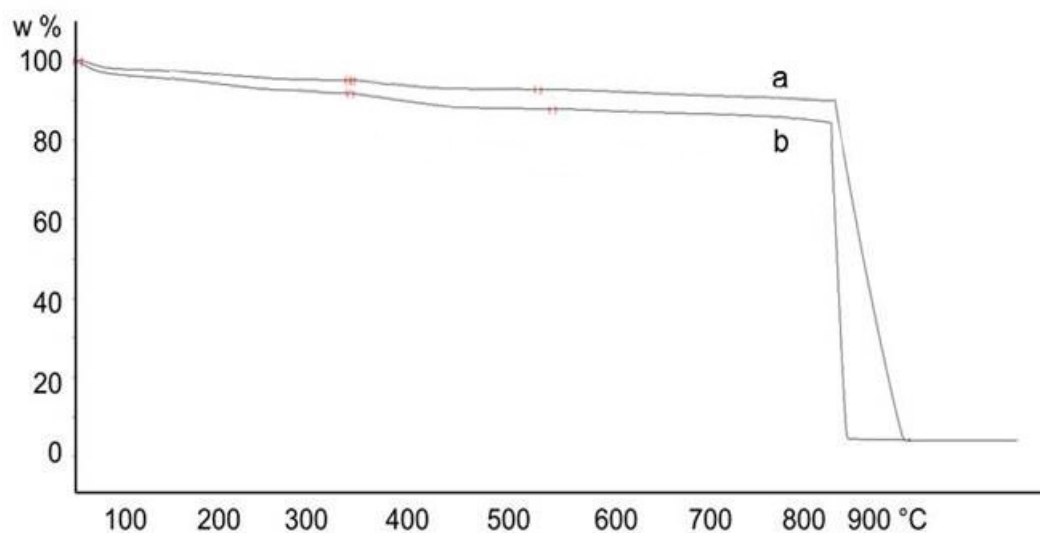


**Figure S7.** TGA curves of G-OH (a) and G-CHO (b).

The amount of functional groups in the adducts was estimated evaluating the mass loss in the temperature range from 150°C to 700°C. The data are collected in Table S2.

**Table S2.** Mass loss for HSAG, G-OH and G-CHO adducts, from TGA analysis.

Sample	Mass loss [%]			
	T < 150°C	150°C < T < 700°C	> 700°C	Residue
HSAG	1.4	1.8	96.8	/
G-OH	3.0	2.9	90.2	4.1
G-CHO	2.6	7.3	89.0	0.1

By comparing data referring to HSAG, to G-OH and to G-CHO adducts, it appears that the mass loss in the temperature range from 150°C to 700°C is larger for the adducts.

For example the functionalization yield for G-CHO was calculated considering mass losses between 150 to 700°C:

$$\text{Functionalization Yield} = \text{G-CHO}_{(\text{mass loss } 150-700^\circ\text{C})} - \text{G-OH}_{(\text{mass loss } 150-700^\circ\text{C})}$$

Data of functionalization yield are shown in Table S3.

**Table S3.** Yield of functionalization for G-CHO.

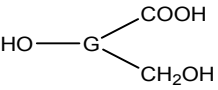
Adduct	Functionalization Yield (%)
--------	-----------------------------

G-CHO	4.4
-------	-----

#### S4. Stoichiometry of the domino Reimer-Tiemann / Cannizzaro process.

Table S4 shows the stoichiometry of the domino Reimer-Tiemann / Cannizzaro process, which leads to the introduction on graphene layers of CH<sub>2</sub>OH and COOH functional groups starting from G-OH.

**Table S4.** Theoretical moles of functional groups in G-OH and G-COOH, assuming the occurring of domino Reimer-Tiemann / Cannizzaro process

Compound	Functional group				
	OH	CHO	CH <sub>2</sub> OH	COOH	COOR
HO—G	2	0	0	0	0
	2	0	1	1	0

According to such domino process, starting from 2 moles of phenolic OH, the Reimer-Tiemann reaction forms two moles of C=O (aldehydes) and the Cannizzaro disproportionation leads to one C=O mole and one OH mole. 2 moles of phenolic OH are still present in G-COOH. The C=O and OH groups after the Cannizzaro reaction should belong to carboxylic acid and benzyl alcohol.

The OH/COOH ratio for the product obtained by the Cannizzaro reaction, calculated on the basis of the stoichiometry reported in Table S4, is:

$$R_{\text{stoic}} = 2 (\text{phenolic } \underline{\text{O}}\underline{\text{H}}) + 1 (\text{benzylic } \underline{\text{O}}\underline{\text{H}}) + 1 (\text{carboxylic } \underline{\text{C}}\underline{\text{O}}\underline{\text{O}}\underline{\text{H}}) / 1 (\text{carboxylic } \underline{\text{C}}\underline{\text{O}}\underline{\text{O}}) = 4/1.$$

## S5. Reaction of G-OH with KOH / H<sub>2</sub>O / CHCl<sub>3</sub> at 0°C (Procedure 2)

### Experimental procedure

In a round bottomed flask equipped with magnetic stirrer and condenser, KOH powder (3.12 g, 55 mmol), CHCl<sub>3</sub> (1.12 mL, 14 mmol) and H<sub>2</sub>O (0.5 mL) were added in sequence. G-OH (0.5 g) was added to such mixture after few seconds, to avoid chloroform decomposition by alkaline ions, well known problem in Reimer-Tiemann reaction performed on phenol ring. The mixture was stirred at 0°C, for 12 hours. After this time, solvent was removed at reduced pressure. The solid was reduced in fine grains in a mortar with a pestel, transferred into a Falcon™ tube (15mL) and water (10 mL) was added. The suspension was sonicated for 10 minutes and centrifuged at 4000 rpm for 10 minutes (3 times). 0.67 g of black powder were obtained. The reaction product is indicated as G-CHO-COOH.

### Characterization

Characterization of G-CHO-COOH was performed by means of FT-IR and XPS. FT-IR spectra are reported in Figure S8, and wide scan XPS spectra in Figure S9. In these figures, spectra of G-CHO and G-CHO-COOH are compared. Description of spectra of G-CHO are in the text.

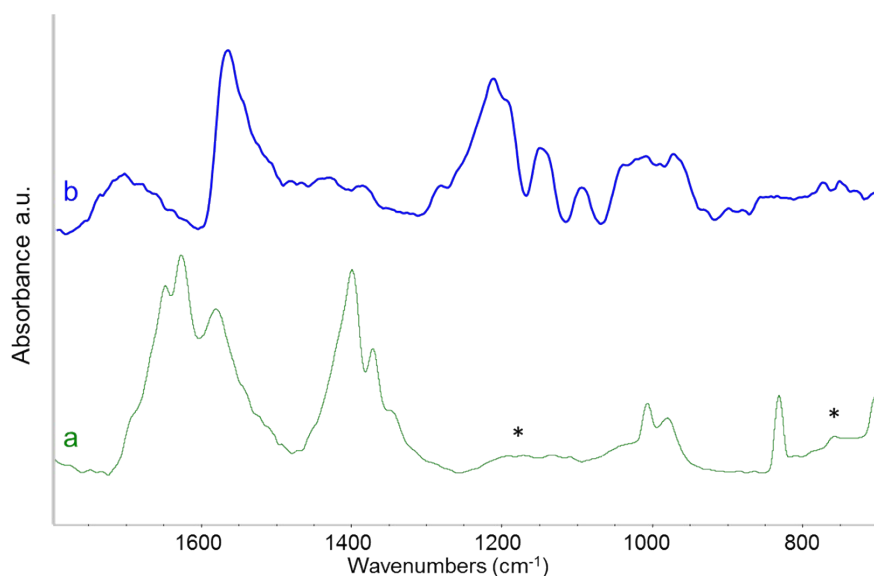


**Figure S8.** FT-IR spectra of G-CHO-COOH (a) and G-CHO (b) in the region 1800-700 cm<sup>-1</sup> after baseline correction. Asterisks indicate absorptions assigned to 2-hydroxyaryl aldehyde functional groups.

The IR spectrum of G-CHO-COOH is dominated by two very strong and structured features: one with peaks at 1668 cm<sup>-1</sup>, 1647 cm<sup>-1</sup>, 1627 cm<sup>-1</sup> and 1578 cm<sup>-1</sup> and the other one with peaks at 1400 cm<sup>-1</sup>, 1372 cm<sup>-1</sup> and 1342 cm<sup>-1</sup>. At lower wavenumbers, it is possible to identify: i) weak

absorptions in the region 1250 - 1100  $\text{cm}^{-1}$  and at 757  $\text{cm}^{-1}$  and ii) four medium bands at 1007  $\text{cm}^{-1}$ , 978  $\text{cm}^{-1}$ , 830  $\text{cm}^{-1}$  and 705  $\text{cm}^{-1}$ . All the strong and medium bands, except for the one at 1578  $\text{cm}^{-1}$  ascribed to the C=C stretching of graphitic moiety enhanced by the polarizing effect of carbonyl groups, can be assigned to the vibrations of potassium hydrogen carbonate. The assignment of the weak bands (in the region 1250-1100  $\text{cm}^{-1}$  and at 757  $\text{cm}^{-1}$ ) is not straightforward. Considering the product of Reimer-Tiemann reaction, a spectral pattern similar to that of salicylaldehyde characterized by the absorption bands due to 2-hydroxyaryl aldehyde group should be expected. From the literature, the IR spectrum of salicylaldehyde shows bands at 1664  $\text{cm}^{-1}$  and 1643  $\text{cm}^{-1}$  (C=O stretching), at 1620  $\text{cm}^{-1}$ , 1580  $\text{cm}^{-1}$ , 1488  $\text{cm}^{-1}$  and 1459  $\text{cm}^{-1}$  (C=C stretching coupled with OH bending and CH bending), at 1450  $\text{cm}^{-1}$  (in plane C-O-H), a sequence in the region 1274-1114  $\text{cm}^{-1}$  (C-OH and C-HO stretching vibrations) and at 753  $\text{cm}^{-1}$  (OH bending) [57]. This data allows the assignment of the weak bands at 753  $\text{cm}^{-1}$  and in the region 1250-1100  $\text{cm}^{-1}$  (marked with asterisks in Figure S8) as due to the presence of 2-hydroxyaryl aldehydes moiety in the G-OH sample. Unfortunately all the other bands result overshadowed by the very strong absorptions of potassium hydrogen carbonate. Findings from IR analysis support the presence of aldehydic functional groups in the product of the reaction performed at 0°C between G-OH and  $\text{CHCl}_3/\text{KOH}$ . The XPS spectra of G-CHO-COOH are shown in Figure S9. Wide scan XPS spectrum of G-CHO-COOH (Figure S9a) exhibits features similar to that of G-COOH, commented in the Text: C and O signals are detected, together with low intensity K and Cl signals. The  $\text{O}_{1s}/\text{C}_{1s}$  atomic ratio is 0.1, which is slightly lower than the ratio of G-CHO (0.12) and slightly higher than that of G-COOH (0.09). The  $\text{C}_{1s}$  envelop (Figure S9b) contains three peaks, attributable to C-C, C-O and C=O, as reported for G-CHO. By performing the deconvolution of  $\text{O}_{1s}$  signal (Figure S9c), two main contributions are identified, i.e. at 531.4 eV and 533 eV, together with two minor components at 530.4 eV and 534.6 eV. The two main signals can be attributed to C=O groups (carbonyl and carboxyl) and to C-O groups (hydroxyl and ether bonded to aromatics), respectively. The latter contribution could account for both phenolic and benzylic OH, but they cannot be separately identified. The signal due to potassium hydrogen carbonate, revealed by IR, should appear at B.E.=289.3  $\pm$  0.6 eV, but is not detectable.

Both IR and XPS analysis of G-CHO-COOH clearly reveal the presence of carbonyls which are assigned by IR to aldehydic functional groups. These findings support the formation of aldehydic derivatives of G-OH, after the reaction with  $\text{CHCl}_3/\text{KOH}$  at 0°C. However, the presence of potassium hydrogen carbonate, shown by IR and not by XPS, needs to be explained, as it is attempted in the next section.

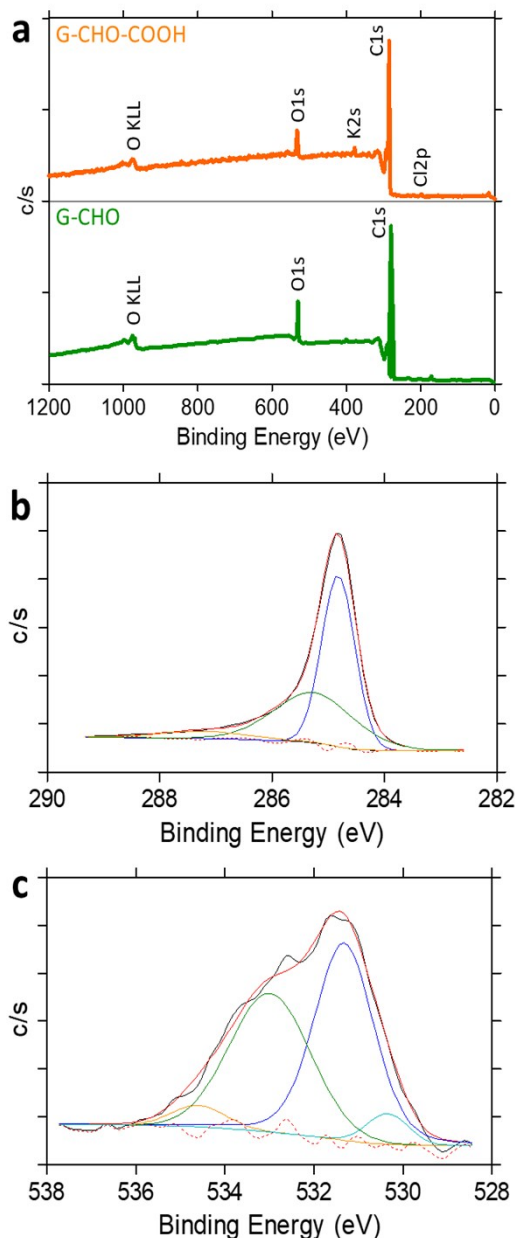


**Figure S9.** XPS analysis of G-CHO-COOH: (a) wide scan spectra of G-CHO-COOH and G-CHO, (b) high resolution C<sub>1s</sub> peak and fitting curves for G-CHO-COOH, (c) high resolution O<sub>1s</sub> peak and fitting curves for G-CHO-COOH.

#### *Mechanism for the formation of G-CHO-COOH*

The mechanism to account for the presence of potassium hydrogen carbonate is tentatively proposed in Figure S10.

It is hypothesized that dichlorocarbene reacts with phenoxide; the O-alkylated product **11** either decomposes or reacts to form ortho-formic products. The decomposition of the dichloro ether **12** in a basic medium allows us to obtain the starting phenol system, potassium hydrogen carbonate and KCl, the latter salt being able to form crystals detected in a WAXD spectrum.

$\text{KHCO}_3$  was not detected in XPS spectra. One can suppose that the purification processes easily remove the potassium salt from the surface probed by photoelectrons, while it remains detectable in between the stacked layers and it is revealed by IR (transmission mode). It is worth recalling that O-alkylations are favoured at low temperatures, compared to C-alkylations. The mechanism in Figure S10 suggests that, at  $0^\circ\text{C}$ , the reaction of dichlorocarbene does not lead to the most thermodynamically stable product but rather occurs under kinetic control.

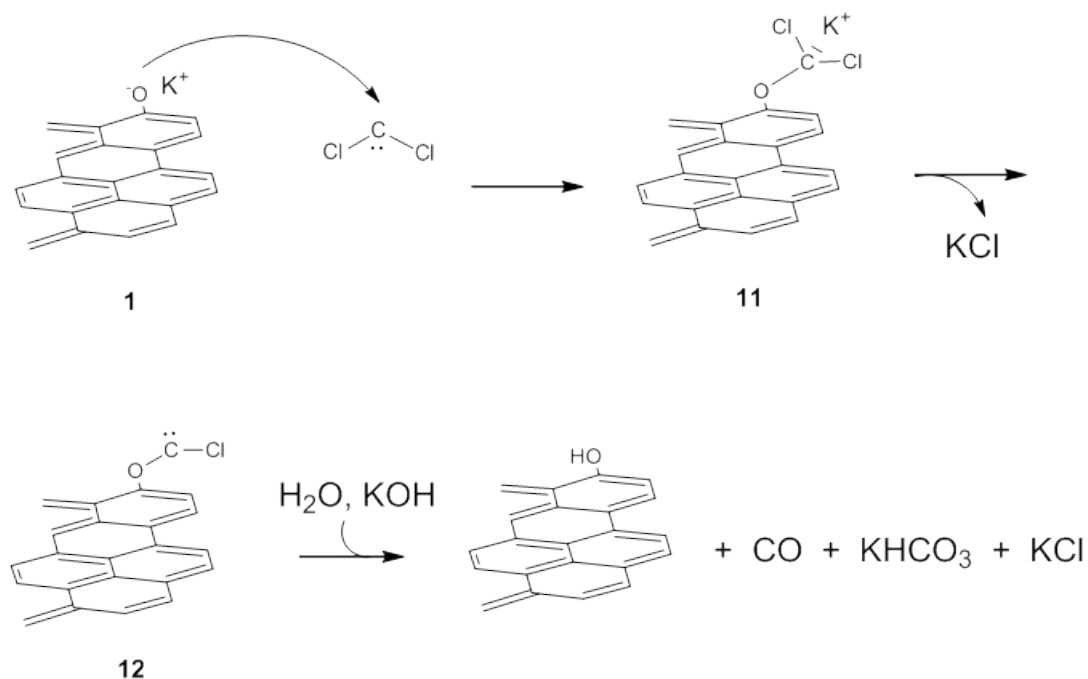


**Figure S10.** Proposed synthetic pathway for the reaction of G-OH with  $\text{CHCl}_3/\text{KOH}$  at  $0^\circ\text{C}$ .

## S6. Crosslinking of G-CHO with hexamethylenediamine

### *Experimental procedure*

G-CHO (0.4 g) and 1,6-hexamethylene diamine (0.03 g) were sonicated for 1 hour. After this time the mixture was left to stir for 12 hours at room temperature. The mixture was washed with dichloromethane (8 mL) and after filtrated under reduce pressure.

### *Characterization*

Infrared spectrum is shown in Figure S11: typical spectral features of aldehyde cannot be detected.

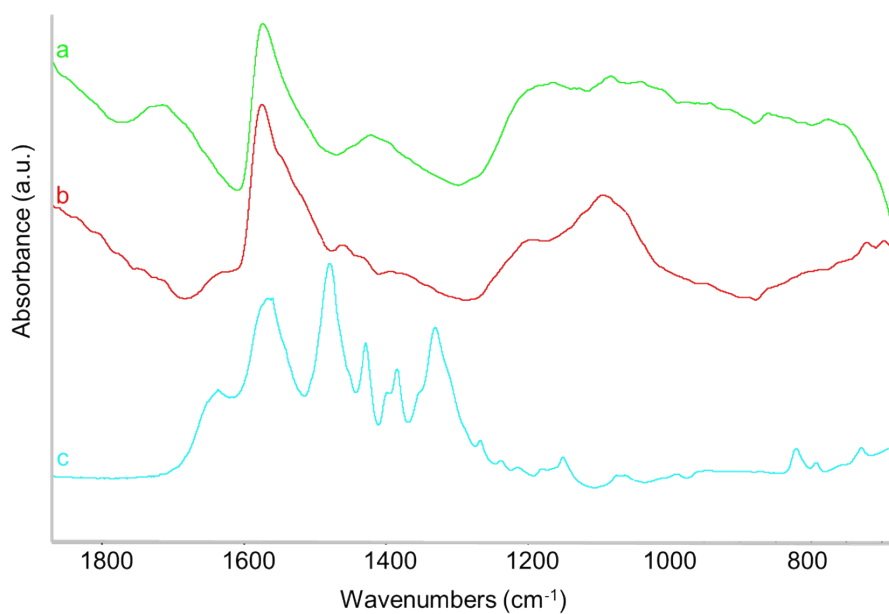


**Figure S11.** FTIR spectra of G-CHO (a), G-OH/HMA (b) and HMA (c) in the region 1800-700 cm<sup>-1</sup>.

## S7. Cyclic Voltammetry (CV)

### *Method:*

Electrochemical measurements Cyclic Voltammetry were conducted in a divided three-electrode cell controlled by a Potentiostat Galvanostat model 2549 (Amel Instrument). A Platinum wire/AgCl 3M reference and a Pt wire auxiliary electrode were used respectively throughout the work. A Glassy Carbon electrode (GC) was used as the working electrode. The electrodes were dried in air prior to electrochemical characterization. The potential was cycled from -0.35 V to +1.0 V at a scan rate of 0.1 V s<sup>-1</sup> in an aqueous solution of 0.1 M Et<sub>4</sub>NBF<sub>4</sub>/10 mM K<sub>4</sub>Fe(CN)<sub>6</sub>. G-CHO water suspension was 0.125 mM.

Electrical properties of G-OH and G-CHO were investigated by cyclic voltammetry. Curves are shown in Figure S.12 a-c.

Results from G-OH were already reported [51]. In this manuscript are reported results obtained with G-CHO. CV measurements were performed on 0.1 M Et<sub>4</sub>NBF<sub>4</sub>/10 mM K<sub>4</sub>Fe(CN)<sub>6</sub> solution (a), on a 0.125 mM G-CHO suspension/0.1 M Et<sub>4</sub>NBF<sub>4</sub> (b) and on the 0.1 M Et<sub>4</sub>NBF<sub>4</sub>/10 mM K<sub>4</sub>Fe(CN)<sub>6</sub> solution, in the presence of 0.125 mM G-CHO.

The expected cyclic voltammogram was obtained for K<sub>4</sub>Fe(CN)<sub>6</sub>. G-CHO did not bring about any detectable signal. This finding could be attributed to the low amount of functional groups on the graphitic substrate. The curves obtained for the Et<sub>4</sub>NBF<sub>4</sub> / K<sub>4</sub>Fe(CN)<sub>6</sub> / G-CHO suspension indicate that G-CHO is able to modify the behavior of redox pairs. Similar results were obtained with G-OH [51].

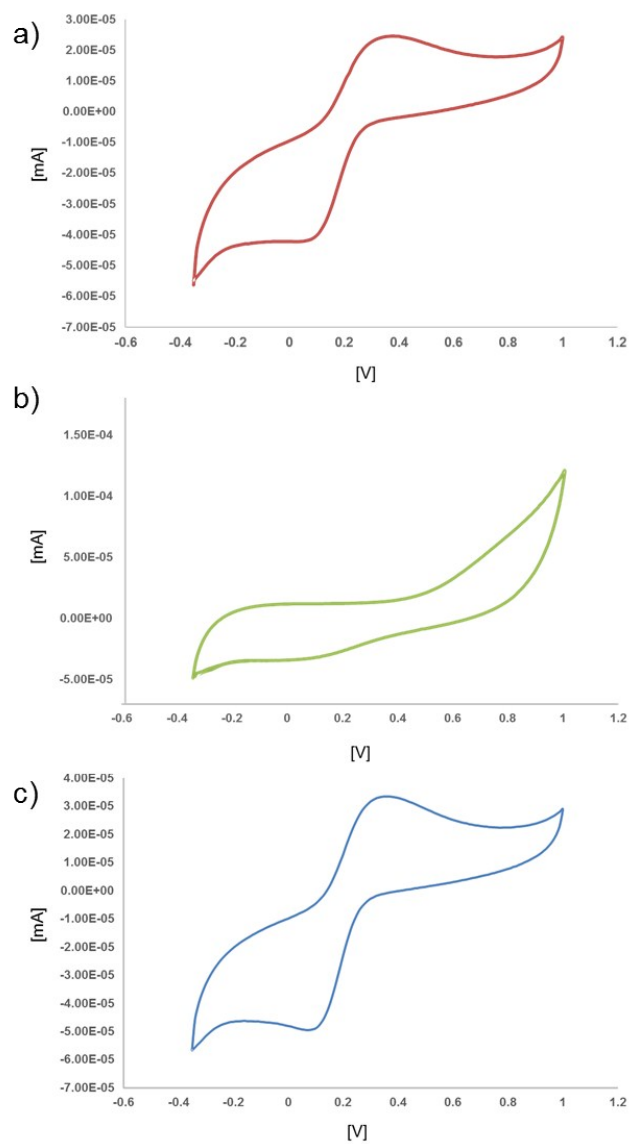


**Figure S12.** CVs of 0.1 M  $\text{Et}_4\text{NBF}_4/10 \text{ mM K}_4\text{Fe}(\text{CN})_6$  solution (a), 0.125 mM G-CHO suspension/0.1 M  $\text{Et}_4\text{NBF}_4$  (b) and 0.1 M  $\text{Et}_4\text{NBF}_4/10 \text{ mM K}_4\text{Fe}(\text{CN})_6$  solution and 0.125 mM G-CHO (c)